Isolation of a Novel Protein Tyrosine Phosphatase Inhibitor, 2-Methyl-Fervenulone, and Its Precursors from *Streptomyces*

Haishan Wang,[†] Kah Leong Lim,[‡] Su Ling Yeo,[§,||] Xiaoli Xu,[⊥] Mui Mui Sim,[†] Anthony E. Ting,[||] Yue Wang,[⊥] Sidney Yee,[§] Y. H. Tan,[§] and Catherine J. Pallen*[,‡]

Medicinal and Combinatorial Chemistry Laboratory, Cell Regulation Laboratory, Lead Discovery Group, Microbial Collection and Screening Laboratory, and Screening for Novel Inhibitors Group, Institute of Molecular and Cell Biology, 30 Medical Drive, Singapore 117609, Singapore

Received June 9, 2000

High-throughput screening identified an extract from *Streptomyces* sp. IM 2096 with inhibitory activity toward several protein tyrosine phosphatases (PTPs). Four 1,2,4-triazine compounds 2096A−D (**1**−**4**) were isolated from this extract and their structures elucidated by interpretation of spectroscopic data and confirmed by degradation and synthesis. The novel glycocyamidine derivatives **1** and **2** are diastereomers and may interconvert. Both are inactive in the PTP inhibition assay. Compounds **1** and **2** are unstable and partially decompose to **3** and glycocyamidine (**5**) at room temperature. Compound **3**, known as MSD-92 or 2-methyl-fervenulone, is a broad-specificity PTP inhibitor with comparable potency to vanadate. The imidazo[4,5-*e*]-1,2,4-triazine (**4**), inactive in the PTP-inhibition assay, may be a degradation product of **3**.

Covalent modification by tyrosine phosphorylation is a major mechanism for regulating the functions of proteins involved in multiple aspects of cellular, physiological, and pathogenic processes. It is reversibly controlled through the dynamic actions of protein tyrosine kinases (PTKs) and phosphatases (PTPs). Numerous and specific inhibitors of PTKs have been isolated and tested as therapeutic agents against human diseases.[1] The large diversity of the PTP superfamily and the demonstrated roles of several PTPs as positive regulators of cellular signaling pathways and in certain human diseases,[2−5] indicate that these phosphatases are promising targets for therapeutic manipulation.

We have taken the approach of using high-throughput screening of actinomycetes extracts to identify novel PTP inhibitors. Actinomycetes have proved to be a valuable source of antibiotics and other bioactive compounds.[6] Furthermore, the PTP inhibitors dephostatin[7] and two phosphatoquinones[8] have been previously isolated from Actinomycetes. Here we report the identification, isolation, and characterization of a known antibiotic, 2-methyl-fervenulone (2096C), as a novel PTP inhibitor, and describe the structures of its novel precursors and a proposed degradation product.

Results and Discussion

Microtiter plate-based screening of 12 000 actinomycete extracts for inhibitory activity toward PTPα identified 40 extracts that inhibited *para*-nitrophenyl phosphate (*p*NPP) and phosphotyrosyl RR-src peptide dephosphorylation by >70% and >60%, respectively. One extract, 2096, reproducibly exerted >60% inhibition on PTPα and on other PTPs subsequently tested, including TCPTP, LAR, PTPβ, and PTPϵ (data not shown), and was selected for further purification.

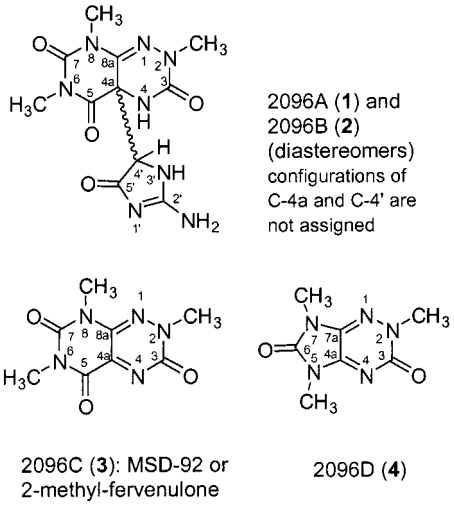

The fermentation broth of *Streptomyces* sp. IM 2096 was freeze-dried and extracted with MeOH. The extracts were fractionated by Si gel column chromatography (eluted with hexanes/EtOAc, CH_2Cl_2/MeOH, MeOH, and MeOH/H_2O). The bioassay-active fractions were combined and resolved by reversed-phase HPLC purification (C_{18}, MeOH/H_2O) to give 2096A (**1**) and 2096B (**2**) as pale yellow solids. These two semi-pure fractions (ca. 85−95% pure as estimated by HPLC at 300 nm) showed good PTPα inhibitory activity. These two compounds are thermally unstable, and the partially decomposed or degraded samples were further purified by reversed-phase HPLC (C_{18}, MeOH/H_2O, 0.1% TFA) to provide, in addition to the TFA salts of **1** and **2**, a polar yellow fraction and a more polar colorless fraction. The compounds 2096C (**3**) and 2096D (**4**) were isolated from the yellow fraction by preparative TLC (EtOAc/CH_2Cl_2/MeOH). Glycocyamidine (**5**, TFA salt) was obtained from the more polar fraction by simple evaporation.

Compounds **1** and **2** did not contain sulfur (MS) or phosphorus (^{31}P NMR) and had the same nominal molecular weight (ESI, $[M + H]^+$ *m*/*z* 323). Their NMR spectra were very similar, therefore, only the interpretation of the spectra of **1** will be discussed in the following text. The ^{1}H

* To whom correspondence should be addressed. Tel.: (65) 874-3742. Fax: (65) 779-1117. E-mail: mcbcp@imcb.nus.edu.sg.
[†] Medicinal and Combinatorial Chemistry Laboratory.
[‡] Cell Regulation Laboratory.Present address for K.L.L.: Department of Pathology, Harvard Medical School, Rm 439, Building D2, 200 Longwood Ave, Boston, MA 02115.
[§] Lead Discovery Group.
[⊥] Microbial Collection and Screening Laboratory.
[||] Screening for Novel Inhibitors Group.

10.1021/np000293+ CCC: $19.00
Published on Web 11/08/2000

Table 1. ^{1}H, ^{13}C, and ^{15}N NMR Data for 2096A (**1**)[a]

	^{13}C NMR		^{1}H NMR		^{15}N NMR[b]	
no.	base[c]	salt[d]	base[c]	salt[d]	base[c]	salt[d]
N-1					285.3	286.0
N2-CH_3	36.4	36.4	3.12	3.12	130.9	130.8
3	149.4	148.9				
N4-H			7.46	8.17	81.3	77.4
4a	60.6	60.4				
5	164.3	162.9				
N6-CH_3	28.2	28.5	3.06	3.09	143.9	142.7
7	149.6	149.4				
N8-CH_3	30.2	30.4	3.09	3.17	108.7	107.4
8a	134.8	133.3				
N-1′				10.13		
2′	173.0[e]	160.6				
2′-NH_2			7.17	9.14		87.2
			7.85	9.43		
N-3′			8.02	9.39	84.7	86.9
4′	65.2	62.8	4.05	4.65		
5′	182.8	171.1				

[a] Measured in DMSO-d_6 at 295 K, all the ^{1}H peaks are singlets. [b] Data obtained from HSQC and HMBC experiments. [c] Base = neutral or free base. [d] Salt = TFA salt. [e] Not visible in 1D ^{13}C NMR, obtained from HMBC experiment.

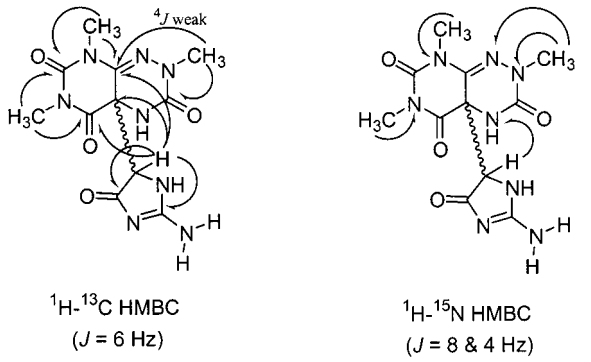

Figure 1. HMBC correlations (arrows) for 2096A (**1**).

NMR of **1** in DMSO-d_6 showed four exchangeable proton signals at δ 8.02, 7.85, 7.46, 7.17 and four nonexchangeable singlets with D_2O at δ 4.05 (1H), 3.06 (3H), 3.09 (3H), and 3.12 (3H). No cross-peak between any two of the above peaks was found in the COSY experiment. The ^{13}C NMR and DEPT spectra suggested **1** had 11 carbons: three methyl groups, one methine, one quaternary carbon, and six other quaternary carbons in a range of amide or amidine-type carbons (Table 1). The ^{1}H−^{13}C HMQC experiment assigned the CH_3 and CH signals. Connectivity of the partial structure was established by ^{1}H−^{13}C HMBC experiment (optimal J = 6 Hz) cross-peaks (Figure 1). As the NMR information obtained from ^{1}H and ^{13}C nuclei was not enough to provide the entire connectivity, ^{1}H−^{15}N HSQC (heteronuclear single quantum correlation spectroscopy) and HMBC experiments[9] were performed. The HSQC spectra showed two cross-peaks [H-4 (δ 7.46)/N-4 (δ 81.3); H-3′ (δ 8.02)/N-3′ (δ 84.7)], the other two active protons provided no cross-peak as they were too broad. The HMBC experiments (optimal J = 8 and 4 Hz) showed more cross-peaks [H-4′ (δ 4.05)/N-4 (δ 81.3); N-2 CH_3 (δ 3.12)/N-1 (δ 285.3) and N-2 (δ 130.9); N-8 CH_3 (δ 3.09)/N-8 (δ 108.7); N-6 CH_3 (δ 3.06)/N-6 (δ 143.9)]. The ^{15}N peak at δ 285.3 suggested the existence of a pyridine-like nitrogen (=N−). Clearly, compound **1** had a structure of a two-ring system with a side chain. As the molecular weight of **1** was an even number (322), with the possible formula suggested as $C_{11}H_{14}N_{6+x}O_y$, only X = 2 with Y = 4 satisfies the requirement. HRESIMS further confirmed the formula $C_{11}H_{14}N_8O_4$ ($[M + H]^+$, m/z 323.1222, calcd for $C_{11}H_{15}N_8O_4$, 323.1216).

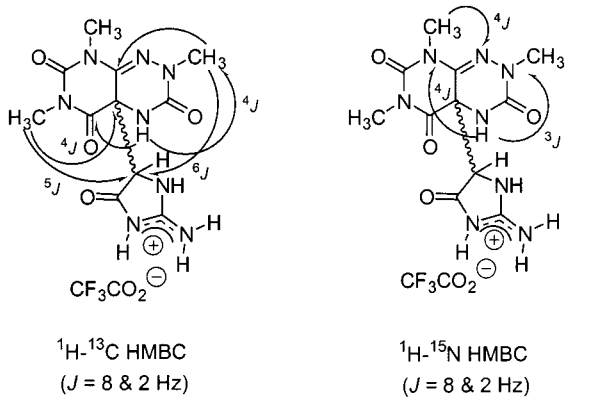

Figure 2. HMBC correlations (arrows) for the TFA salt of 2096A (**1**).

Table 2. ^{1}H, ^{13}C, and ^{15}N NMR Data for 2096B (**2**)[a]

	^{13}C NMR		^{1}H NMR		^{15}N NMR[b]	
no.	base[c]	salt[d]	base[c]	salt[d]	base[c]	salt[d]
N-1					279.8	283.1
N2-CH_3	36.4	36.4	3.13	3.13	132.1	130.8
3	150.3	149.3				
N4−H			7.41	8.05	81.3	78.6
4a	59.2	60.0				
5	162.9	161.9				
N6-CH_3	28.2	28.6	3.01	3.09	142.0	142.0
7	149.6	149.5				
N8-CH_3	29.9	30.2	3.15	3.17	111.0	109.1
8a	136.3	134.1				
N-1′				10.60		
2′	172.6[e]	160.1				
2′-NH_2			7.17	9.45		87.0
			7.85	(3H)		
N-3′			8.02		85.7	
4′	64.4	63.5	4.17	4.72		
5′	183.2	170.5				

[a] Measured in DMSO-d_6 at 295 K, all the ^{1}H peaks are singlets. [b] Data obtained from HSQC and HMBC experiments. [c] Base = neutral or free base. [d] Salt = TFA salt. [e] Not visible in 1D ^{13}C NMR, obtained from HMBC experiment.

The two "invisible" nitrogen atoms not detected in the ^{15}N NMR spectra are most likely to be in the other moiety, which has the formula $C_3H_4N_3O$. Among all possible structures, the formula $C_3H_4N_3O$ best matched the residue derived from glycocyamidine[10] (**5**) with respect to the NMR data. The suggested structure for **1** is shown in Figure 1. To confirm the structure of **1**, the TFA salt of **1** was further investigated with ^{1}H−^{15}N HSQC experiments, which led us to confirm that the protonated form of glycocyamidine residue had the structure shown in Figure 2 (data listed in Table 2). The ^{1}H−^{13}C and ^{1}H−^{15}N HMBC experiments, (optimal J = 8 and 2 Hz) of the TFA salt of **1** gave more connectivity information than that of the free base. With optimal J = 2 Hz, the ^{1}H−^{13}C HMBC showed good correlation through 4, 5, even 6 bonds; the ^{1}H−^{15}N HMBC experiments also showed very important correlations through ^3J and ^4J. Compounds **1** and **2** (Table 2) have similar NMR spectra and data; **2** is the diastereomer of **1**, and they can interconvert. This is due to the acidic 4′-H, which causes epimerization to occur easily. As a result, the two chiral centers at C-4a and C-4′ are not assigned.

Compounds **1** and **2** are soluble in DMSO, MeOH, and H_2O, but insoluble in CH_2Cl_2, $CHCl_3$, and hexanes. They are unstable in solutions (H_2O, MeOH, DMSO) and slowly decompose to a yellow fluorescent compound. After washing the partially decomposed **1** and **2** with CH_2Cl_2, the soluble yellow fraction was separated from **1** and **2**. The crude yellow fraction was purified by preparative TLC to give **3** and **4**.

Table 3. ^{1}H, ^{13}C, and ^{15}N NMR Data for 2096C (**3**) at 295 K

	^{13}C NMR		^{1}H NMR		^{15}N NMR[a]	
no.	$CDCl_3$	DMSO-d_6	$CDCl_3$	DMSO-d_6	$CDCl_3$	DMSO-d_6
N-1					323.2	314.6
N2-CH_3	42.1	41.2	3.91	3.74	187.3	181.9
3	150.8	152.6				
N-4						
4a	143.6	145.1				
5	157.0	157.8				
N6-CH_3	29.7	28.7	3.51	3.33	155.3	152.6
7	148.9	149.2				
N8-CH_3	29.6	28.9	3.54	3.34	109.8	110.5
8a	137.0	137.7				

[a] Data obtained from HMBC experiments.

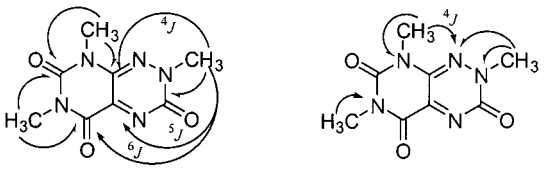

^{1}H-^{13}C HMBC (J = 6 Hz, $CDCl_3$ J = 2 Hz, DMSO-d_6)

^{1}H-^{15}N HMBC (J = 4 Hz, $CDCl_3$ J = 2 Hz, DMSO-d_6)

Figure 3. HMBC correlations (arrows) for 2096C (**3**).

Table 4. ^{1}H, ^{13}C and ^{15}N NMR Data for 2096D (**4**) at 295 K

	^{13}C NMR		^{1}H NMR		^{15}N NMR[a]	
no.	$CDCl_3$	DMSO-d_6	$CDCl_3$	DMSO-d_6	$CDCl_3$	DMSO-d_6
N-1					293.3	288.1
N2-CH_3	40.8	39.9	3.74	3.56	166.7	163.8
3	154.4	153.5				
N-4						231.9
4a	150.2	150.6				
N5-CH_3	26.0	25.3	3.37	3.160	121.8	122.8
6	153.6	153.8				
N7-CH_3	26.1	25.7	3.34	3.163	105.2	106.5
7a	133.3	134.0				

[a] Data obtained from HMBC experiments.

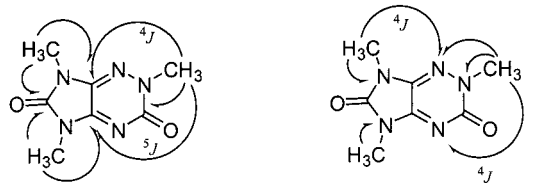

^{1}H-^{13}C HMBC (J = 6 Hz, $CDCl_3$; J = 2 Hz, DMSO-d_6)

^{1}H-^{15}N HMBC (J = 4 Hz, $CDCl_3$; J = 2 Hz, DMSO-d_6)

Figure 4. HMBC correlations (arrows) for 2096D (**4**).

The molecular formula of **3** was confirmed as $C_8H_9N_5O_3$ by HREIMS ([M]$^+$, m/z 223.0713, calcd 223.0705) or by HRESIMS ([M + H]$^+$, m/z 224.0787, calcd for $C_8H_{10}N_5O_3$, 224.0784). Its NMR data are listed in Table 3, and its structure was elucidated by using a combination of ^{1}H and ^{13}C NMR, ^{1}H−^{13}C HMQC, HMBC, and ^{1}H−^{15}N HMBC experiments (Figure 3). Compound **3** was confirmed to be the known antibiotic: MSD-92 or 2-methyl-fervenulone.[11]

The molecular formula of **4** was confirmed as $C_7H_9N_5O_2$ by HREIMS ([M]$^+$, m/z 195.0756, calcd 195.0756). Its structure was also elucidated by a combination of ^{1}H, ^{13}C NMR; ^{1}H−^{13}C HMQC; HMBC, and ^{1}H−^{15}N HMBC experiments (Table 4, Figure 4). The structure of **4** was similar to that of **3**, but with a C═O missing from the C-5 position.

Scheme 1

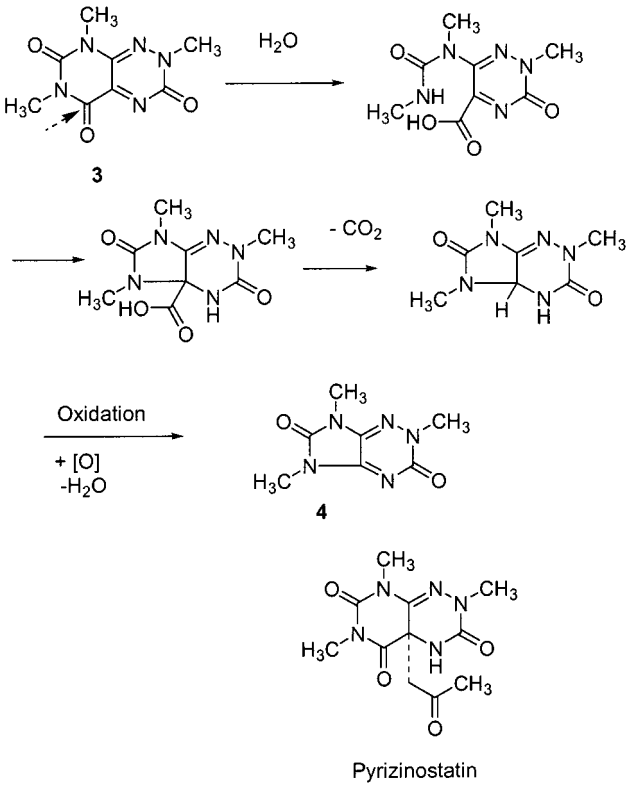

Scheme 2

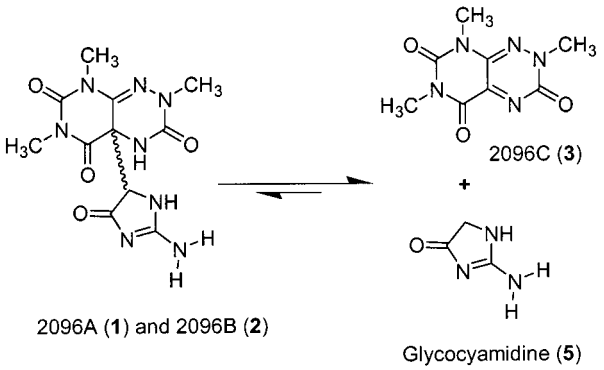

A mechanistic pathway based on the breakdown of the C-5 and N-6 bond[12] was proposed to explain the formation of **4** from **3** (Scheme 1).

Compounds **1** and **2** are similar in structure to the known pyroglutamyl peptidase inhibitor pyrizinostatin.[13] Pyrizinostatin has the same two-ring system (compound **3**) but with a ketone side chain. Both **1** and **2** are optically active. It is possible that **1** and **2** are enantioselectively synthesized by the microorganism starting from **3** and **5** (Scheme 2). Direct analysis of fresh fermentation broth by HPLC showed that **1** and **2** naturally exist, while **3** was not observed (or below the detectable level). Upon storage, and during the isolation and purification process, decomposition predominates. The stability experiment showed that, after incubating at 52 °C for 4 h, the amounts of **1** and **2** were reduced by 62% and 85%, respectively, in the aqueous solution. The formation of **3** was verified by HPLC analysis. Formation of **5** was also confirmed by NMR. In a DMSO-d_6 solution of partially decomposed **1** or **2**, free **5** was identified by the appearance of a proton at δ 3.60, and it correlates with carbon at δ 49.8 (CH_2) in HMQC experiment and with carbons at δ 187.4 and δ 173.0 in the HMBC spectrum. Compound **5** was purified by HPLC and con-

Table 5. Activities of Protein Phosphatases in the Presence of 1 μM Compounds **3**, **4**, and Sodium Orthovanadate[a]

phosphatase	[nM]	**3**	**4**	Na_3VO_4
Yop	0.1	10 ± 1.0	95 ± 4.0	14 ± 1.0
ϵD1D2	1.0	17 ± 4.0	99 ± 1.0	18 ± 2.0
CD45	1.0	15 ± 2.5	96 ± 1.0	14 ± 0.5
TCPTP	1.0	34 ± 1.0	99 ± 2.0	31 ± 5.0
αD1D2	5.0	17 ± 1.1	98 ± 0.5	24 ± 1.5
LAR-D1	5.0	17 ± 2.0	97 ± 1.5	26 ± 1.0
λPP	5.0	48 ± 2.0	100 ± 6.0	49 ± 3.0
CIP	0.5	100 ± 1.0	99 ± 4.0	98 ± 3.0

[a] Reactions were carried out as described in the Experimental Section; [nM] refers to the concentration of phosphatase assayed. Numbers indicate percentage activities relative to respective control reactions without addition of **3**, **4**, or Na_3VO_4. Numbers represent the average of the activities measured with three separate enzyme preparations, each of which was assayed in duplicate ± S.D.

verted to its HCl salt. The ^{1}H and ^{13}C NMR data of isolated **5**, as its hydrochloric acid salt, are identical to those of the synthetic product and are comparable to those reported.[14] With the structures of two degradation products (**3** and **5**) as additional proof, the structures of **1** and **2** are determined to be 4a-(2-amino-5-oxo-4,5-dihydro-3*H*-imidazol-4-yl)-2,4,4a,8-tetrahydro-2,6,8-trimethyl-pyrimido[5,4-*e*]-1,2,4-triazine-3,5,7(6*H*)-triones, and the structure of **4** is 2,5,7-trimethyl-2,7-dihydro-5*H*-imidazo[4,5-*e*]-1,2,4-triazine-3,6-dione.

Bioassay demonstrated that **3** is a potent PTP inhibitor (see below). Compounds **1** and **2** were much weaker inhibitors, but were found by HPLC analysis to be contaminated with ca. 6−10% of **3**. The TFA salts of **1** and **2** were further purified by washing with CH_2Cl_2 to remove trace amounts of **3**. The fresh solution of **1** and **2** (TFA salt, the amount of **3** was estimated below 1 mol % by HPLC analysis) are inactive, but became active after prolonged storage. It is clear that **3** is responsible for the activity of **1** and **2**.

The effects of **3** and **4** on the in vitro activities of several members of the PTP superfamily, representing receptor and nonreceptor tyrosine-specific PTPs that utilize an active site cysteine in catalysis,[15] were investigated. At 1 μM, **3** inhibited all the PTPs tested, while **4**, a proposed degradation product of **3**, had negligible effects on PTP activity (Table 5). Although all receptor PTP catalytic domains (ϵD1D2, CD45, αD1D2, and LAR-D1) were inhibited to a similar extent (83−85%), the degree of inhibition exerted by **3** on the nonreceptor PTPs tested was more variable, with about 65% inhibition observed for TC-PTP and 90% for Yop. To examine whether **3** could inhibit the activity of phosphatases not belonging to the PTP superfamily, λPP and the nonspecific alkaline phosphatase calf intestine phosphatase (CIP) were assayed in the presence or absence of compounds **3** or **4**. λPP is a dual specificity phosphatase closely related to Types 1 and 2 serine/threonine phosphatases but with the ability to dephosphorylate phosphotyrosyl proteins[16,17] as well. Although λPP's activity was inhibited about 50% by **3**, it was unaffected by **4**. Neither compound had any detectable effect on the *p*NPP phosphatase activity of CIP (Table 5). Reactions with CIP were performed at a neutral pH instead of a slightly acidic pH used in the measurements of the other enzymes. At this pH, though **3** has no effects on CIP activity, it continues to behave as a PTP inhibitor for both Yop and αD1D2 (results not shown), ruling out the possibility that the neutral environment plays a role in nullifying the inhibition by **3** on phosphatase activity. Thus, the inhibitory action of **3** is specific to protein tyrosine phosphatases, but is not exclusive to those employing an active-site cysteine residue in their catalytic mechanism. In side-by-side reactions, **3** inhibited the PTPs to almost the same extent as the classical PTP-inhibitor vanadate does[18,19] (Table 5). The virtually indistinguishable effects of **3** and vanadate also extended to the dual specificity λPP, as well as to their lack of effect on CIP.

At 50 μM or 100 μM, **3** showed no antimicrobial activity against *Mycobacterium smegmatis*, *Staphylococcus aureus*, *Escherichia coli*, *Enterococcus faecalis*, *Proteus vulgaris*, *Pseudomonas aeruginosa*, *Candida albicans*, or *Curvualaria* sp.

Experimental Section

General Experimental Procedures. TLC was carried out on precoated plates: analytical (Merck Kieselgel 60 F_{254}), spots visualized with UV light; preparative-scale (Aldrich, silica, 1 mm thick). Flash column chromatography was performed with silica (Merck, 70−230 and 230−400 mesh). Optical rotations were measured with a JASCO DIP-1000 digital polarimeter. Infrared spectra (IR) were recorded with a Perkin-Elmer 1600 series FTIR (film or KBr pellet). All the 1D and 2D NMR experiments for ^{1}H (400.13 MHz), ^{13}C (100.61 MHz), and ^{15}N (40.55 MHz) nuclei were obtained on a Bruker AVANCE-400 digital NMR spectrometer. ^{1}H−^{13}C and ^{1}H−^{15}N 2D experiments (HMQC, HSQC, and HMBC) were run with *Z*-gradient selection. ^{1}H and ^{13}C chemical shifts are expressed in ppm (δ) relative to internal TMS, ^{15}N (40.55 MHz) chemical shifts were obtained from 2D experiments and are calibrated with 80% $MeNO_2$ in $CDCl_3$ as 380.2 ppm. HRMS spectra were determined using a VG Micromass 7035E instrument (EI) and a PerSeptive Biosystems Mariner TOF spectrometer (ESI). Analytical HPLC was performed on a Hewlett-Packard 1050Ti series equipped with a diode array detector, using a C_{18} column (ODS Hypersil, 5 μm, 4.6 × 250 mm) and linear gradient elution (flow rate, 1.0 mL/min; solvent A, 0.1% TFA in H_2O; solvent B, 0.1% TFA in MeOH; solvent B increased from 5% to 60% in 20 min and then from 60% to 100% in additional 5 min).

Actinomycetes Extracts. Approximately 2000 different strains of actinomycetes were fermented in six different types of 10-mL liquid media for 7 days at 30 °C. Each culture, with its cells and supernatant, was extracted by adding an equal amount of 100% methanol and incubating overnight at 30 °C. The extracts were filtered, and the filtrates were freeze-dried in 2-mL aliquots for long-term storage at −70 °C.

Isolation and Taxonomy of the Actinomycete Strain IM 2096. The procedures for the isolation and taxonomic characterization of the strain IM 2096 were as described by Wang et al.[20] The actinomycete strain IM 2096, from which **3** was purified, was isolated from a soil sample collected in the Singapore Botanic Garden. Its colony exhibits properties characteristic of *Streptomyces* on ISP 4 medium plate. Both aerial and substrate mycelia were well developed. At maturity, straight chains with more than 20 spores were formed on the aerial mycelium. The color of the aerial mycelium was white and that of the substrate mycelium was light brown. No diffusible pigment was produced on ISP 2, ISP 3, ISP 4, and Bennett medium plates. The cell-wall peptidoglycans contained a major amount of L-diaminopimelic acid. The complete nucleotide sequence of the 16S rRNA gene of IM 2096 was determined for phylogenetic analysis. IM 2096 was found to have the closest phylogenetic relationship with *Streptomyces albulus*, and the 16S rRNA gene sequences are 97% identical between the two organisms. On the basis of morphological, chemotaxonomic, and phylogenetic evidence, we assigned the actinomycete strain IM 2096 to the genus *Streptomyces*.

High-Throughput Screens. High-throughput screens for inhibitory activity toward PTPα were performed in 96-well plates (Nunclon). Dephosphorylation of the substrate (*p*NPP) was measured in 180-μL reactions/well in assay buffer containing 50 mM of sodium acetate (pH 5.5), 0.5 mg/mL of BSA,

and 0.5 mM dithiothreitol. The purified enzyme PTPα (0.3 μg/well) and extracts (5 μL in 50% methanol) were preincubated for 5−10 min at room temperature in a volume of 170 μL. Reactions were initiated by adding 10 μL of substrate in assay buffer to a final concentration of 2 mM. For each plate, six reference control wells containing PTPα were preincubated with 5 μL 50% methanol at the same time as the test samples. As a positive control for PTPα inhibition, 1 μM Na_3VO_4, a potent inhibitor of PTPs, was added to some wells. Blank wells contained 5 μL 50% MeOH, 2 mM *p*NPP in assay buffer, and no enzyme. For each set of experiments (from 2 to 5 plates), reference controls in a separate plate were read at different time points to check the linearity of the reaction. Reactions were stopped with 25 μL of KH_2PO_4 after 45−60 min incubation at room temperature. The plates were read immediately in a multilabel counter (Wallac 1420 Victor). The optical density (OD_{405}) of the reference wells ranged between 0.7 and 1.2, which represents <10% conversion of the substrate and falls within the linear part of the reaction. Percentage inhibition was determined using the formula: % Inhibition = [{-(OD ref-OD blank) − (OD test-OD blank)}/(OD ref-OD blank)] × 100.

Phosphatase Assays. The expression, purification, quantitation, and storage of bacterially expressed PTPα, PTPϵ, and PTPβ have previously been described.[21,22] All other PTPs described in the text were purchased from New England Biolabs. Dephosphorylation of *p*NPP was measured in 450-μL reactions containing 50 mM sodium acetate (pH 5.5, or pH 7 for CIP), 0.5 mg/mL of BSA, 0.5 mM of dithiothreitol, and 2 mM of *p*NPP. Reactions with λPP also contained 2 mM Mn^{2+}. The RR-src peptide was phosphorylated and used at 2.5 μM in reactions with PTPα, as described.[21,22] All reactions were carried out at 30 °C and terminated during the linear portion of the reaction.

Purification Procedures. The bioassay-active fermentation broth (4 L) was freeze-dried. The solid residue was extracted with MeOH (2.5 L × 2), 10% H_2O in MeOH (2 L × 2), and 20% H_2O in MeOH (1 L × 3) at room temperature. The bioassay-active extracts were combined and concentrated under reduced pressure below 35 °C. The wet residue (about 1/3 of the total) was first mixed with Si gel (70−230 mesh) and freeze-dried, then applied on a Si gel (230−400 mesh) column. The column (internal diameter, 6 cm; sample layer height, 4.5 cm; fine silica layer, 6 cm) was eluted with EtOAc in hexanes (0%, 250 mL; 50%, 250 mL; 100%, 250 mL × 2), MeOH in CH_2Cl_2 (0%, 250 mL × 2; 50%, 250 mL × 2; 90%, 250 mL × 2; 100%, 250 mL × 3), 10% H_2O in MeOH (250 mL × 2). The active fractions (usually the 10−90% MeOH in CH_2Cl_2) were combined and evaporated below 30 °C under reduced pressure.

The above residue was further fractionated either by a semipreparative Waters 600E system equipped with a 990 PDA, using a Prep Nova-Pak HRC_{18} column (6 μm, 7.8 mm × 300 mm, flow rate 2 mL/min, solvent MeOH/ H_2O) or by a Waters Delta Prep 4000 system equipped with a 996 photodiode array detector, using Prep Nova-Pak HRC_{18} column segments (6 μm, 25 mm × 310 mm; flow rate, 21.2 mL/min; solvent A = H_2O, B = MeOH; 0−5 min, 5% B, 5−30 min, 5% to 30% B, linear gradient, 30−40 min, 100% B). Fractions corresponding to different peaks were freeze-dried. Two of them were found active in the bioassay, they were named as 2096A (**1**, 105 mg, overall yield from the 4 L of fermentation broth) and 2096B (**2**, 73 mg).

The isolated **1** and **2** were unstable and contained ca. 6−10% of 2096C (**3**) by HPLC analysis. The latter can be removed and isolated by simply washing **1** and **2** with CH_2Cl_2. Compounds **1** and **2** can also be further purified by HPLC (25 mm × 310 mm column, flow rate, 20 mL/min, MeOH/H_2O containing 0.1% TFA) to give their TFA salts. The purification also provided a polar yellow fraction (mainly **3**) and a more polar fraction, confirmed as glycocyamidine by ESIMS.

Crude **3** obtained from washing **1** and **2** with CH_2Cl_2 and HPLC fraction was purified by preparative TLC (silica; EtOAc/MeOH/CH_2Cl_2, 30:9:1, developed twice) to give **3** (12 mg) and 2096D (**4**, 5 mg).

4a-(2-Amino-5-oxo-4,5-dihydro-3*H*-imidazol-4-yl)-2,4,-4a,8-tetrahydro-2,6,8-trimethyl-pyrimido[5,4-*e*]-1,2,4-triazine-3,5,7(6*H*)-triones (1 and 2). 2096A (1) TFA Salt: The salt contains TFA salt of **2**, the ratio of **1**:**2** is 90.1:9.9 (by HPLC at 300 nm): yellow powder, $[\alpha]^{33}_D$ −10.5 (*c* 1.0, MeOH); IR (KBr) 3380−3210 (br), 1783, 1724 (strong), 1676 (strong), 1540, 1440, 1382, 1203, 1139, 1024 cm^{-1}; UV (MeOH/H_2O/0.1%TFA, PDA) λ_{max} 295 nm; retention time (analytical HPLC) 14.3 min; NMR data, see Table 1.

2096B (2) TFA Salt. The salt contains TFA salt of **1**, the ratio of **1**:**2** is 32.3:67.7 (by HPLC at 300 nm); yellow powder, $[\alpha]^{33}_D$ +2.8 (*c* 1.0, MeOH); IR (KBr) 3390−3193 (br), 1785, 1724 (strong), 1676 (strong), 1540, 1441, 1382, 1203, 1139, 1024 cm^{-1}; UV (MeOH/H_2O/0.1%TFA, PDA) λ_{max} 302 nm; retention time (analytical HPLC) 13.3 min; NMR data, see Table 2; HRESIMS *m*/*z* 323.1219 ($[M + H]^+$, calcd 323.1216 for $C_{11}H_{15}N_8O_4$).

2,8-Dihydro-2,6,8-trimethyl-pyrimido[5,4-*e*]-1,2,4-triazine-3,5,7(6*H*)-trione (2096C, 3): yellow solid; IR (KBr) 3568, 3536, 3435, 3380, 2963, 2935, 1728, 1694 (strong), 1666 (strong), 1615, 1541, 1473, 1437, 1385, 1328, 1312, 1247, 1032 cm^{-1}; UV (MeOH/H_2O/0.1%TFA, PDA) λ_{max} 238, 417 nm; retention time (analytical HPLC) 10.0 min; NMR data, see Table 3. The ^1H NMR, UV, and IR data comparable with those reported.[11a]

2,5,7-Trimethyl-2,7-dihydro-5*H*-imidazo[4,5-*e*]-1,2,4-triazine-3,6-dione (2096D, 4): pale yellow solid; IR (film) 3433, 1767, 1679, 1622, 1510, 1465, 1338, 1201, 1020 cm^{-1}; UV (MeOH/H_2O/0.1%TFA, PDA) λ_{max} 260, 325 nm; retention time (analytical HPLC) 11.0 min; NMR data, see Table 4.

Glycocyamidine (5) HCl Salt. To the HPLC fraction of glycocyamidine, HCl (1 N) was added to give **5** in the HCl salt form (5 mg): white solid, ^1H NMR (DMSO-d_6) δ 12.20 (br s, 1H), 9.49 (s, 1H), 9.04 (br s, 1H), 8.82 (br s, 1H), 4.11 (s, 2H); ^{13}C NMR (DMSO-d_6) δ 172.8, 158.5, 48.1; $^1H-^{13}C$ HMQC δ_H 4.11/δ_C 48.1; $^1H-^{13}C$ HMBC δ_H 4.11/δ_C 172.8, 158.5. TFA salt: HRESIMS *m*/*z* 122.0358 ($[M + Na]^+$, calcd 122.0330 for $C_3H_5N_3ONa$), 199.0951 ($[2M + H]^+$, calcd 199.0943 for $C_6H_{11}N_6O_2$), 221.0747 ($[2M + Na]^+$, calcd 221.0763 for $C_6H_{10}N_6O_2Na$). Its NMR spectra are identical to those of synthetic **5**·HCl [obtained by refluxing the guanidineacetic acid with 6 N HCl[10a] for 6 days: ^1H NMR (DMSO-d_6) δ 4.14 (s); ^{13}C NMR (DMSO-d_6) δ 172.9, 159.0, 48.5 and comparable with those reported.[14]

Acknowledgment. We thank Hwei Fern Leong and Hong He for excellent technical assistance with high throughput screening and large-scale fermentation. This work was supported by the National Science and Technology Board of Singapore.

Supporting Information Available: ^1H and ^{13}C NMR spectra of 2096A−D **1**−**4**. This material is available free of charge via the Internet at http://pubs.acs.org.

References and Notes

(1) Al-Obeidi, F. A.; Wu, J. J.; Lam, K. S. *Biopolymers* **1998**, *47*, 197−223.
(2) Hooft van Huijsduijnen, R. *Gene* **1998**, *225*, 1−8.
(3) Streuli, M. *Curr. Op. Cell Biol.* **1996**, *8*, 182−188.
(4) Neel, B. G.; Tonks, N. K. *Curr. Op. Cell Biol.* **1997**, *9*, 193−204.
(5) Li, L.; Dixon, J. E. *Semin. Immunol.* **2000**, *12*, 75−84.
(6) Sanglier, J. J.; Wellington, E. M. H.; Behal, V.; Fiedler, H. P.; Ghorbel, R. E.; Finance, C.; Hacene, M.; Kamoun, A.; Kelly, C.; Mercer, D. K.; Prinzis, S.; Trigo, C. *Res. Microbiol.* **1993**, *144*, 661−663.
(7) Imoto, M.; Kakeya, H.; Sawa, T.; Hayashi, C.; Hamada, M.; Takeuchi, T.; Umezawa, K. *J. Antibiot.* **1993**, *46*, 1342−1346.
(8) Kagamizono, T.; Hamaguchi, T.; Ando, T.; Sugawara, K.; Adachi, T.; Osada, H. *J. Antibiot.* **1999**, *52*, 75−80.
(9) (a) Levy, G. C.; Lichter, R. L. *Nitrogen-15 Nuclear Magnetic Resonance Spectroscopy*; John Wiley & Sons: New York, 1979. (b) Wang, H.; Ganesan, A. *J. Org. Chem.* **2000**, *65*, 1022−1030. (c) Martin, G. E.; Hadden, C. E. *J. Nat. Prod.* **2000**, *63*, 543−585.
(10) (a) Bengelsdorf, I. S. *J. Am. Chem. Soc.* **1953**, *75*, 3138−3140. (b) Matsumoto, K.; Rapoport, H. *J. Org. Chem.* **1968**, *33*, 552−558. (c) Kenyon, G. L.; Rowley, G. L. *J. Am. Chem. Soc.* **1971**, *93*, 5552−5560.

(11) (a) Miller, T. W.; Chaiet, L.; Arison, B.; Walker, R. W.; Trenner, N. R.; Wolf, F. J. *Antimicrob. Agents Chemother.* **1963**, 58−62. (b) Taylor, E. C.; Sowinski, F. *J. Am. Chem. Soc.* **1969**, *91*, 2143-2144. (c) Taylor, E. C.; Sowinski, F. *J. Org. Chem.* **1975**, *40*, 2321−2329. (d) Ichiba, M.; Nishigaki, S.; Senga, K. *J. Org. Chem.* **1978**, *43*, 469−472.
(12) Werner-Simon, S.; Pfleiderer, W. *J. Heterocyclic Chem.* **1996**, *33*, 949−960.
(13) (a) Aoyagi, T.; Hatsu, M.; Imada, C.; Naganawa, H.; Okami, Y.; Takeuchi, T. *J. Antibiot.* **1992**, *45*, 1795−1796. (b) Hatsu, M.; Naganawa, H.; Aoyagi, T.; Takeuchi, T.; Kodama, Y. *J. Antibiot.* **1992**, *45*, 1961−1962.
(14) Olofson, A.; Yakushijin, K.; Horne, D. A. *J. Org. Chem.* **1998**, *63*, 5787−5790.
(15) Zhang, Z. Y. *Crit. Rev. Biochem. Mol. Biol.* **1998**, *33*, 1−52.
(16) Cohen, P. T. W.; Cohen, P. *Biochem. J.* **1989**, *260*, 931−934.
(17) Zhuo, S.; Clemens, J. C.; Hakes, D. J.; Barford, D.; Dixon, J. E. *J. Biol. Chem.* **1993**, *268*, 17754−17761.
(18) Swarup, G.; Cohen, S.; Garbers, D. L. Biochem. *Biophys. Res. Commun.* **1982**, *107*, 1104−1109.
(19) Huyer, G.; Liu, S.; Kelly, J.; Moffat, J.; Payette, P.; Kennedy, B.; Tsaprailis, G.; Gresser, M. J.; Ramachandran, C. *J. Biol. Chem.* **1997**, *272*, 843−851.
(20) Wang, Y.; Zhang, Z.; Ruan, J.; Wang, Y.; Ali, S. M. J. *Ind. Microbiol. Biotech.* **1999**, *23*, 178−187.
(21) Wang, Y.; Pallen, C. J. *EMBO J.* **1991**, *10*, 3231−3237.
(22) Lim, K. L.; Lai, D. S. Y.; Kalousek, M. B.; Wang, Y.; Pallen, C. J. *Eur. J. Biochem.* **1997**, *245*, 693−700.

NP000293+